KIRTLANDIA®

The Cleveland Museum of Natural History

Febrnary 1996 *Number 49:19-43*

STENOSTEUS ANGUSTOPECTUS SP. NOV. FROM THE CLEVELAND SHALE (FAMENNIAN) OF NORTHERN OHIO WITH A REVIEW OF SELENOSTEID (PLACODERMI) SYSTEMATICS

ROBERT K. CARR
Department of Biological Sciences
Ohio University
Athens, Ohio 45701

ABSTRACT

A new species of *Stenostens* Dean, *Stenostens angustopectns,* is described from the Cleveland Shale (Famennian) of northern Ohio and is based on material recovered from the Interstate 71 Paleontological Salvage Project. *Stenostens angustopectus* is characterized by: (1) long and narrow posterior ventrolateral plates, (2) a narrow median process on the anterior ventrolateral plate, (3) a tongue-in-groove joint between the anterior lateral and anterior dorsolateral plates, (4) a posterodorsal process on the suborbital plate, and (5) a posterior superognathal plate lamina that posteriorly is rotated 90°. This new species provides informative comparative material for a reevaluation of Dean's original descriptions of *Stenosteus glaber* and *Selenostens brevis,* which were based on incomplete single specimens preserved in part and counterpart. *Stenosteus* and *Selenosteus* are retained as distinct genera. Uniting these two taxa are the denticulation pattern of the inferognathal and a relative reduction of the central plate length. *Stenostens* and *Selenosteus* are united with *Gymnotrachelns* and *Melanosteus* based on the presence of a stem-like prehypophysial region of the parasphenoid plate and a loose connection between the dermal cheek and head shield. Finally, Selenosteidae *sensn* Lelièvre, Feist, Goujet, and Blieck is retained (the relationships of *Brannosteus* remain unresolved).

Introduction

Several authors have evaluated the phylogenetic relationships among eubrachythoracid arthrodires (coccosteomorph and pachyosteomorph arthrodires) including members of the subgroup Selenosteidae Dean, 1901 (e.g., see Miles and Dennis, 1979; Lelièvre et al., 1987; Gardiner and Miles, 1990, 1994; Carr, 1991, 1994). These evaluations have attempted to determine the relationships of North American, European, and Australian taxa; however, many of the North American forms lack a clear diagnosis or are based on fragmentary material thereby limiting the phylogenetic resolution within previous studies. Addressing this problem, Carr (1991, 1994) analyzed two North American taxa (*Heintzichthys gouldii* and *Gymnotrachelus hydei,* respectively). This paper provides a further analysis of poorly known North American taxa.

Dean (1901) described two aspinothoracid arthrodires (*seusu* Miles and Dennis, 1979), *Selenosteus brevis* and *Stenosteus glaber,* from the Cleveland Shale of Ohio; each was based on a single specimen preserved in part and counterpart. Analyses of these taxa are problematic due to a lack of additional material and poor preservation. Dunkle and Bungart described several additional aspinothoracid arthrodires from the Cleveland Shale fauna (*Gymnotrachelus,* 1939, see Carr, 1994, for a redescription; *Holdenius,* 1942; and *Paramylostoma,* 1945), but this material also is based on disarticulated and incomplete specimens. Inadequate material continues to limit systematic analyses of the Cleveland Shale fauna. In addition, the relationships between North American and other aspinothoracid arthrodires remain unclear. Fundamental to any systematic review are a phylogenetic diagnosis of *Selenosteus* and *Stenosteus* and the description of undescribed Cleveland Shale material. This paper describes a new species of *Stenosteus, Stenosteus angustopectus*, from the Cleveland Shale that provides the basis for a reevaluation of the holotypes for *Selenosteus brevis* and *Stenosteus glaber.* Finally, the new material augments Dean's (1901) original description and figures.

Anatomical abbreviations used in figures and listed at the end of the paper follow those of Dennis-Bryan (1987) and Carr (1991). Specimen number prefixes denote their respective institutions: CMNH, Cleveland Museum of Natural History, Cleveland, Ohio; and AMNH, American Museum of Natural History, New York City. The suffix "id" when used to form taxonomic adjectives does not refer to the familial level in Linnean classification, but is used as a convenience for discussing informal taxonomic units.

Systematic Paleontology

Class Placodermi McCoy, 1848
Order Arthrodira Woodward, 1891
Family Selenosteidae Dean, 1901
(*sensu* Lelièvre et al., 1987)
Genus *Stenosteus* Dean, 1901
Stenosteus angustopectus sp. nov.
Figures 1–17

Name

L. *augnstus* — narrow; L. *pectus* — breast, chest. Refers to the narrow ventral thoracic shield.

Diagnosis

Stenosteus angustopectus is a selenosteid arthrodire characterized by: (1) long and narrow posterior ventrolateral plates, (2) a narrow median process on the anterior ventrolateral plate, (3) a tongue-in-groove joint between the anterior lateral and anterior dorsolateral plates, (4) a posterodorsal process on the suborbital plate, and (5) a posterior superognathal plate whose posterior lamina is rotated 90°.

Holotype

CMNH 8042 (Figures 1, 2, 5–8, 11, 13, 15, 16). The specimen possesses an incomplete head shield in external view with the pineal and rostral plates missing, a complete cheek assembly, anterior and posterior ventrolateral plates, an anterior dorsolateral plate, and fragmented posterior median ventral, median dorsal, possible posterior dorsolateral, and parasphenoid plates.

Additional Material

CMNH 8041: suborbital plates, inferognathal, sclerotics, posterior superognathals, and perichondral ossifications. CMNH 8043 (Figures 9, 11, 13, 14, 15, 17): incomplete head shield, inferognathals, incomplete cheek with sclerotics, incomplete thoracic shield with anterior median ventral plate, and scapulocoracoid. CMNH 8044 (Figures 1, 3, 7, 12): incomplete head shield with isolated rostral, complete cheek assembly with sclerotics, lateral thoracic plates, perichondral ossifications, but lacking ventral plates and median dorsal plate. The left marginal and paranuchal plates are preserved in internal view. CMNH 8045 (Figures 1, 2, 7): complete head shield in external view, inferognathals, fragmented and incomplete thoracic shield, incomplete cheek with sclerotics, and perichondral ossifications. CMNH 8046 (Figures 4, 10): incomplete head shield in internal view with an isolated rostral plate (lacking gnathal plates and parasphenoid), cheek with sclerotics, and incomplete thoracic shield. CMNH 9598: anterior ventrolateral plates, impression of the posterior suborbital plate, and fragmented posterior median ventral plate and scapulocoracoid. CMNH 9931: posterior ventrolateral plate.

Table 1 documents the presence of diagnostic characters used to relate the referred material to *Stenosteus angustopectus.* Several equivocal characters (equivocal at a level capable of resolving the relationships of *Selenosteus*

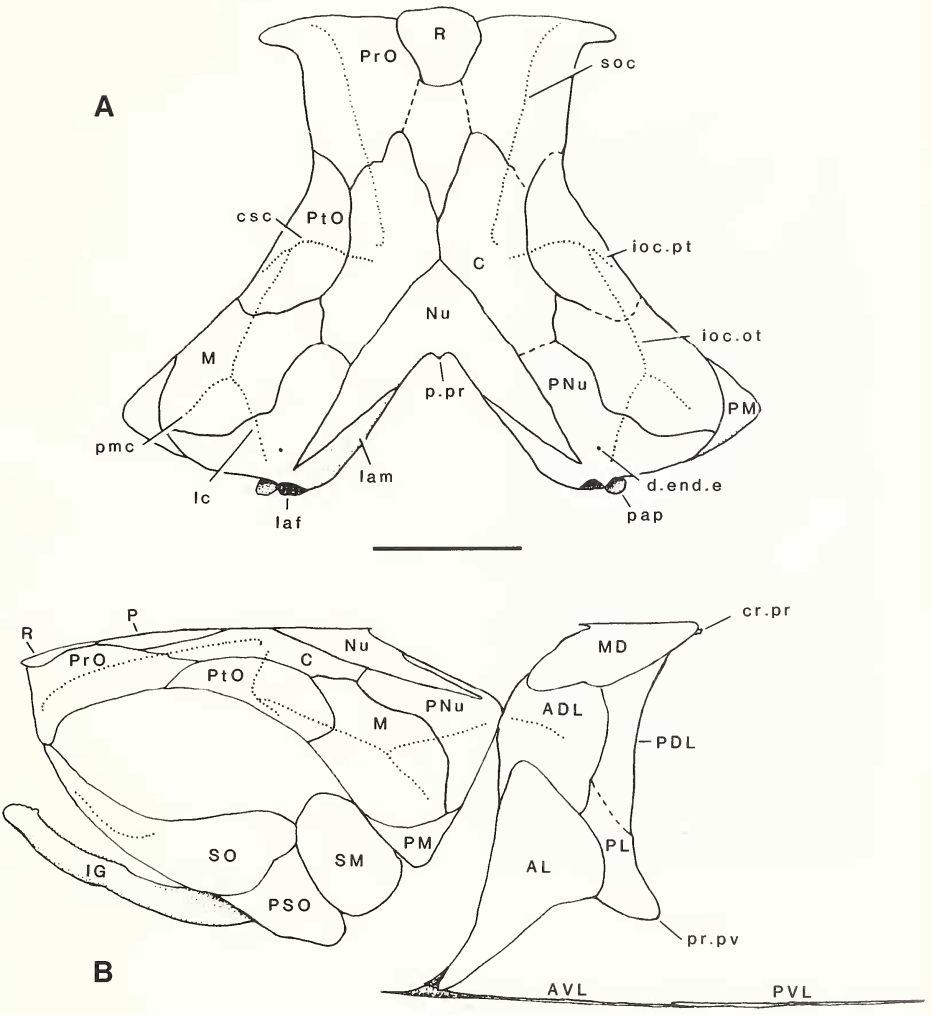

Figure 1. *Stenosteus angustopectus* sp. nov. A, a reconstruction of the head shield in dorsal view. Based on a composite of photographic tracings from CMNH 8042, CMNH 8044, and CMNH 8045. The reconstruction portrays the secondary flattening seen in all the specimens. B, a reconstruction of the head and thoracic shields in left lateral view. Scale bar = 5 cm.

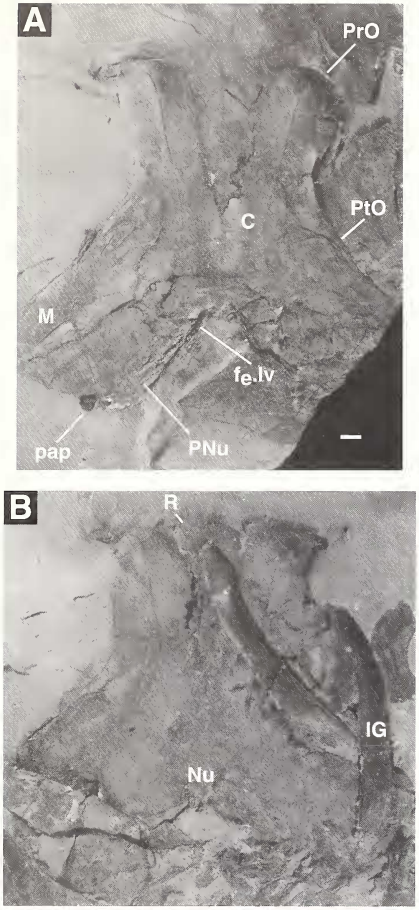

Figure 2. *Stenosteus angustopectus* sp. nov. A, head shield of holotype (CMNH 8042) in dorsal view and B, head shield of CMNH 8045 in dorsal view. Scale bar = 1 cm.

and *Stenosteus* to other selenosteids) are included to distinguish *Stenosteus* specimens from *Seleuosteus*. There are no contradictory features between the referred material and *Stenosteus angustopectus*.

Occurrence

The holotype and referred material was collected by field crews from the Cleveland Museum of Natural History during the Interstate 71 Paleontological Salvage Project (1966–1967). Specimens were recovered from the Cleveland Shale at the intersection of West 130th Street and Interstate 71, Cleveland, Ohio.

Stratigraphy

The Cleveland Shale is in the Famennian Stage of the Devonian System. The *Stenosteus angustopectus* material was taken from the *Heintzichthys gouldii* zone formerly exposed in a quarry located at West 130th Street and Interstate 71, which is now filled in and covered by the interstate (Carr, 1991, based on a personal communication from William Hlavin; however, the detailed stratigraphic position for this unit within the Cleveland Shale is unclear). The Cleveland Shale, in the Cleveland area, overlies the Chagrin Shale and is itself overlain by the Bedford Shale.

Description

Head Shield

General features. The head shield (Figures 1–7) is composed of 15 individual plates; three unpaired median plates (rostral, pineal, and nuchal) and six paired plates (preorbital, postorbital, central, marginal, paranuchal, and postmarginal). There is no evidence for the presence of postnasal plates and they are assumed to be lost phylogenetically. All plates are secondarily deformed, that is, flattened during diagenesis. The contact surfaces between adjacent plates are denoted as either a contact face on the visceral surface or an overlap area on the external surface (after Dennis and Miles, 1979a).

Rostral (R). The rostral and pineal plates, as a rule, are sutured weakly to adjacent plates resulting in either their displacement or loss during fossilization with the one exception of CMNH 8045 (missing in the holotype, CMNH 8042). The rostral plate (Figures 1, 2B, 3A) is triangular in shape possessing a broad anterior margin with a shallow descending face. In CMNH 8045 (Figure 2B), the descending face possesses a roughened texture. Overlap patterns are not completely discernible, although a preorbital contact face appears to be present on the internal surface of CMNH 8044 (cf.PrO, Figure 3A). A ventral anterior thickening (a.th, Carr, 1991, fig. 4A) is absent.

Pineal (P). The pineal plate (found in CMNH 8045 only; Figures 1, 2B) separates the preorbital plates and the anterior third of the central plates. The nature of the preorbital-pineal overlap is unclear based on available material. An absence of an apparent pineal contact face on the visceral surface of the rostral plate suggests that the pineal plate overlies the rostral. An external pineal opening is absent (the opening seen in CMNH 8045, Figure 2B, is not centrally located and represents damage to the bone).

Nuchal (Nu). The nuchal plate (Figures 1, 2A, B) is triangular in external view with a deep posterior embayment that in life would have left the posterior neurocranium and

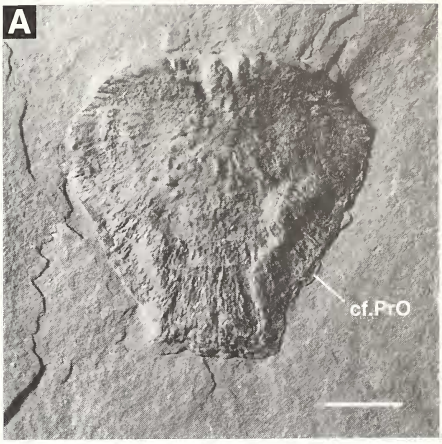

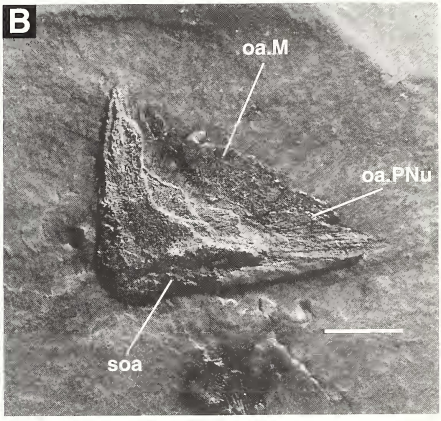

Figure 3. *Stenosteus angustopectus* sp. nov. (CMNH 8044). A, rostral plate in internal view and B, left postmarginal plate in external view. Scale bars = 1 cm.

presumed synarcual articulation exposed, i.e., uncovered by dermal bone. The sides of the embayment form an angle of *ca.* 80° in the holotype (CMNH 8042; CMNH 8045 = *ca.* 100°). A median nuchal process is present (p. pr., Figure 1). The nuchal extends anteriorly between the central plates to the level of their centers of ossification. Posterolateral nuchal alae extend to nearly the posterior margin of the head shield. A shallow shelf lateral to the median process and facing dorsally may represent the site of attachment for the levator muscles of the head (f_c.lv, Figure 2A). The nuchal is not preserved in internal view.

Preorbital (PrO). The preorbital plate (Figures 1, 2A, B) possesses a strongly developed preorbital dermal process. The anterolateral corners of the head shield are downturned (Figure 2) with the body of the rostral plate apparently not participating in a descending face. This downturned condition of the preorbital plate may reflect the compression of the head shield anterior to the internal thickenings of the preorbital dermal process (in *Gymnotrachelus* and *Heintzichthys* the preor-

Table 1. A table of diagnostic characters used to relate the referred material to *Stenosteus angustopectus* sp. nov. A superscript (1) indicates autapomorphic features of *S. angustopectus* based on the holotype, CMNH 8042. A superscript (2) indicates secondary autapomorphic features (missing in the type) that are found in referred specimens with a clear link to the type. Remaining characters represent equivocal features at a higher level of analysis, but provide evidence to distinguish *Stenosteus* specimens from *Selenosteus.* There are no contradictory features between the referred material and *Stenosteus angustopectus* sp. nov. An (X) indicates that the character is preserved in the respective specimen with an empty cell indicating its absence.

Diagnostic Character	8042 (holotype)	8041	8043	8044	8045	8046	9598
PVL[1]	X		X				
AVL process[1]	X					X	X
ADL-AL suture[1]	X		X (AL only)			X	
SO process[1]	X	X	X	X		fragmented	
PSG[1]	X	X					
PL process[2]			X	X			
C-M contact	X		X	X	X		
MD shape	fragmented				X	X	

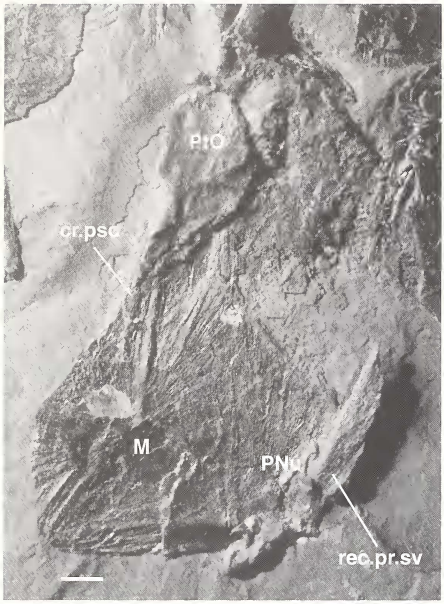

Figure 4. *Stenosteus angustopectus* sp. nov. (CMNH 8046). Right postorbital, marginal, and paranuchal plates in internal view. Scale bar = 1 cm.

bital plate is expanded anteriorly over the rhinocapsular region, Carr, 1994, p. 7, fig. 3). The supraorbital sensory line groove (soc, Figure 1) traverses the preorbital plate terminating medial to the dermal process. The ratio of parasagittal lengths between the preorbital and central plates is *ca.* 0.88 in the holotype (PrO/C, CMNH 8042; CMNH 8045 = *ca.* 0.80) and to the postorbital plate is *ca.* 1.1 (PrO/PtO, CMNH 8042; CMNH 8045 = *ca.* 1.1). The postorbital plate, which lies at an angle to the sagittal plane, is subequal to the preorbital plate when measured along its greatest dimension (PrO/PtO = *ca.* 0.92 and *ca.* 1.04 in CMNH 8045 and 8042 respectively). Internal views are not available.

Postorbital (PtO). The postorbital plate (Figures 1, 2A, B, 4) is narrow (length/width in CMNH 8042 = *ca.* 2.6 and CMNH 8045 = *ca.* 2.7) with a postorbital process absent. There is a subtle convexity along the lateral border of this plate. The grooves for the postorbital (ioc.pt, Figure 1) and otic (ioc.ot, Figure 1) branches of the infraorbital sensory line form a closed angle (less than 45°). A central sensory line groove is present (csc, Figure 1) and terminates before the medial edge of the plate. In CMNH 8045 the central sensory line groove is continuous with its extension onto the central plate.

Internally, CMNH 8046 (Figure 4) possesses a continuation of the supraorbital vault, which is bounded medially by a low ridge. This ridge continues posterolaterally as the posterior supraorbital crista (cr.pso, Figure 4) to the lateral margin of the head and may continue for a very short distance onto the marginal plate. Suture lines between the preorbital and marginal plates are unclear in the one internally exposed specimen (CMNH 8046). If the supraorbital crista does continue onto the marginal plate it is limited to the most anterolateral portion of the plate. Finally, the inframarginal crista extends forward to connect with the supraorbital vault.

Central (C). The central plates (Figures 1, 2A, B) are separated anteriorly by the pineal plate and posteriorly by the nuchal plate reducing the central-central contact to approximately one sixth of their total longitudinal length. Two sensory line grooves are present. A continuation of the groove for the supraorbital sensory line (soc, Figure 1) is present and terminates near the ossification center in a J-shape that opens laterally. A continuation of the central sensory line groove (csc, Figure 1) from the postorbital plate is present bilaterally in CMNH 8042, 8043, and 8045, although distinct and continuous with the central sensory line groove on the postorbital plate only in CMNH 8045. Overlaps are difficult to discern, although the postorbital plates are typically displaced on top of the central plates suggesting the latter are overlapped by the postorbital plates. It appears that the central plates overlap the nuchal plate and preorbital plates (in part). A central-marginal plate contact is present, which is approximately equal to the central plate's length of contact with the paranuchal plate. In CMNH 8045 (Figure 2B), the central and postorbital plates extend anteriorly to a similar level; whereas, in CMNH 8042 (Figure 2A) the central plates project further anteriorly along the medial edge of the preorbital plate. Internal features are not distinguishable on the internally exposed material.

Marginal (M). The marginal plate (Figures 1, 2A, B) is present in the orbital margin (refer to the discussion of Character 3 below) and is in contact with the central plate. Carr (1991) noted that aspinothoracid arthrodires typically lack this contact (e.g., *Heintzichthys, Gorgonichthys,* and *Pachyosteus*) with *Rhinosteus* possessing a contact and *Selenosteus* being polymorphic. The Cleveland Museum of Natural History *"Selenosteus"* material used in the 1991 analysis is assigned here to *Stenosteus.* Continuing onto the marginal plate, the postotic branch of the infraorbital sensory line groove extends to the ossification center. Here, the groove continues as the main lateral line (lc, Figure 1) onto the paranuchal plate. A postmarginal sensory line groove (pmc, Figure 1) extends posterolaterally from the ossification center and terminates before reaching the plate margin. The angle formed by the postmarginal and main sensory line grooves is *ca.* 85–90°. Equidimensional angles are formed by the latter two grooves and the postotic infraorbital line groove (130–135°).

Internally (Figure 4), the inframarginal crista extends

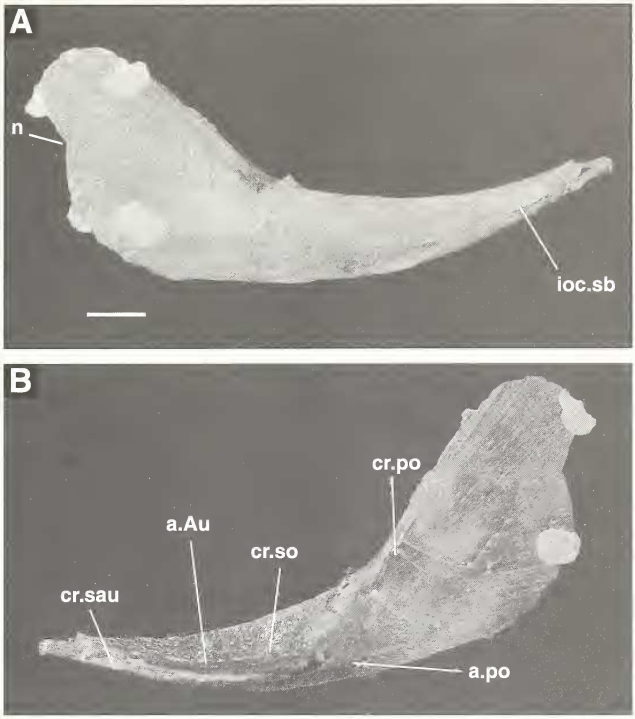

Figure 5. *Stenosteus angustopectus* sp. nov. Right suborbital plate (CMNH 8042) in A, external and B, internal views. Scale bar = 1 cm.

from the margin of the supraorbital vault to the marginal plate ossification center. From there, it extends beneath the postmarginal sensory line groove to the plate margin decreasing in height to the plate's edge. A second thickening extends from the ossification center beneath the main lateral line. As noted above, the supraorbital crista may extend onto the marginal plate. This extension does not necessarily indicate the involvement of the marginal plate in the orbital border (see discussion of Character 3 below).

Postmarginal (PM). The postmarginal plate (Figure 1; present in CMNH 8044, 8045, and 8046; missing in the holotype, CMNH 8042) is triangular in shape with the anteroventral and posterior margins forming an angle of *ca.* 72–80° (Figure 3B). The plate is overlapped by the paranuchal (oa.PNu, Figure 3B) and marginal (oa.M, Figure 3B) plates with the latter forming the larger overlap. A groove for the postmarginal sensory line is absent. The posterior margin is depressed forming a subobstantic area (soa, Figure 3B; Dennis-Bryan, 1987, fig. 5), which appears to be limited to the postmarginal plate. Internally (CMNH 8045), a continuation of the inframarginal crista is absent.

Paranuchal (PNu). The main lateral line groove traverses the paranuchal plate (Figures 1, 4). Medial to the groove, an external endolymphatic pore (d.end.e, Figure 1) is present. A narrow process projects laterally to overlap the postmarginal plate. The posterior plate margin is transverse or slightly convex (in contrast to *Selenosteus brevis* where the margin is embayed). A very small postnuchal process (Carr, 1991, character 30) extends to the tip of the nuchal ala. The postnuchal process is continued as a well-developed shelf on the descending posterior face of the head shield (lam, Figure 1; a similar shelf is seen in *Gymnotrachelus*, Carr, 1994, fig. 5). It is possible that this shelf represents an expansion of the attachment site for the levator muscles of the head. A paraarticular process (pap, Figures 1, 2A) is strongly developed.

Internally (Figure 4), the nuchal thickening is continued laterally along the posteromedial border of the paranuchal

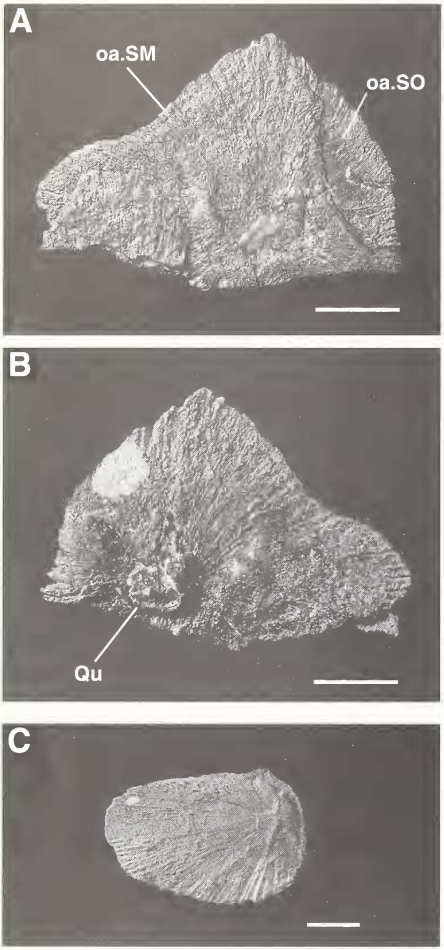

Figure 6. *Stenosteus angustopectus* sp. nov. (CMNH 8042). Right postsuborbital plate in A, external and B, internal views. C, right submarginal plate in internal view. Scale bars = 1 cm.

plate. An additional thickening continues from the articular fossa under the posterolateral ala of the paranuchal plate (along the posterior border toward the postmarginal plate). A distinct depression for the cuccularis muscle is not discernible. Along the paranuchal portion of the transverse occipital arch, a recess for the supravagal process of the neurocranium may be present (rec.pr.sv, Figure 4). It appears as a shallow step since the ventral cover for the recess has been lost.

Cheek Plates

General features. The three paired plates of the cheek (suborbital, posterior suborbital, and submarginal; Figures 5, 6A, B and 6C, respectively) do not fuse to the head shield (a primitive feature of aspinothoracid arthrodires). The ovoid to subrectangular submarginal plate loosely abuts a very small overlap area on the postsuborbital. Its shape is in contrast to the elongate submarginal of basal aspinothoracid arthrodires. The cheek plates are secondarily deformed, that is, flattened during diagenesis.

Suborbital (SO). The shape of the suborbital plate (Figures 1B, 5) is similar to that of other selenosteids with an expanded posterior region ("blade") that tapers gradually to form an anterior suborbital region ("handle"). A notch is seen along the posterior margin (n, Figure 5A) delimiting a posterodorsal process. The suborbital branch of the infraorbital sensory line groove (ioc.sb, Figure 5A) is present; however, it is limited to the "handle" region. The groove parallels the internal autopalatine depression and separates the outer surface into asymmetrical regions with the ventral one being smaller (in contrast to *Gyumotrachelus,* where the ventral region is larger, Carr, 1994). A supraoral sensory line groove is absent.

Internally, subocular (cr.so, Figure 5B), subautopalatine (cr.sau, Figure 5B), and postautopalatine (a.po, Figure 5B; = R3 of Heintz, 1932) cristae and an autopalatine depression (a.Au, Figure 5B) are present on the surface of the "handle" portion. The subautopalatine crista is broken; however, there is no evidence for the presence of a contact face for the posterior superognathal as seen in *Dunkleosteus* and *Eastmanosteus* (Carr, 1991, cf.PSG, fig. 5B; Dennis-Bryan, 1987, figs. 9, 13). A low postocular crista (cr.po, Figure 5B) is present. The postautopalatine posteroventral thickening (a.po, Figure 5B; = R3 of Heintz, 1932) extends a very short distance from the confluence of the other three cristae.

Postsuborbital (PSO). The postsuborbital plate (PSO, Figures 1B, 6A, B) is roughly triangular in outline. Anteriorly there is an overlap area for the suborbital plate (oa.SO, Figure 6A) and posteriorly there is a small and nearly indistinct overlap area for the submarginal plate (oa.SM, Figure 6A). Dorsally, both of these overlap areas approach the plate's apex resulting in little or no separation between the submarginal and suborbital plates (a distinct gap between the suborbital and submarginal plates is present in *Gyumotrachelus*). The postsuborbital plate forms a small notch along the posterior border of the suborbital plate.

Internally, CMNH 8042 possesses a perichondrally ossified quadrate (Qu, Figure 6B) with the condylar region located near the ventral plate margin. The presence of a detent process cannot be determined (Gardiner and Miles, 1990,

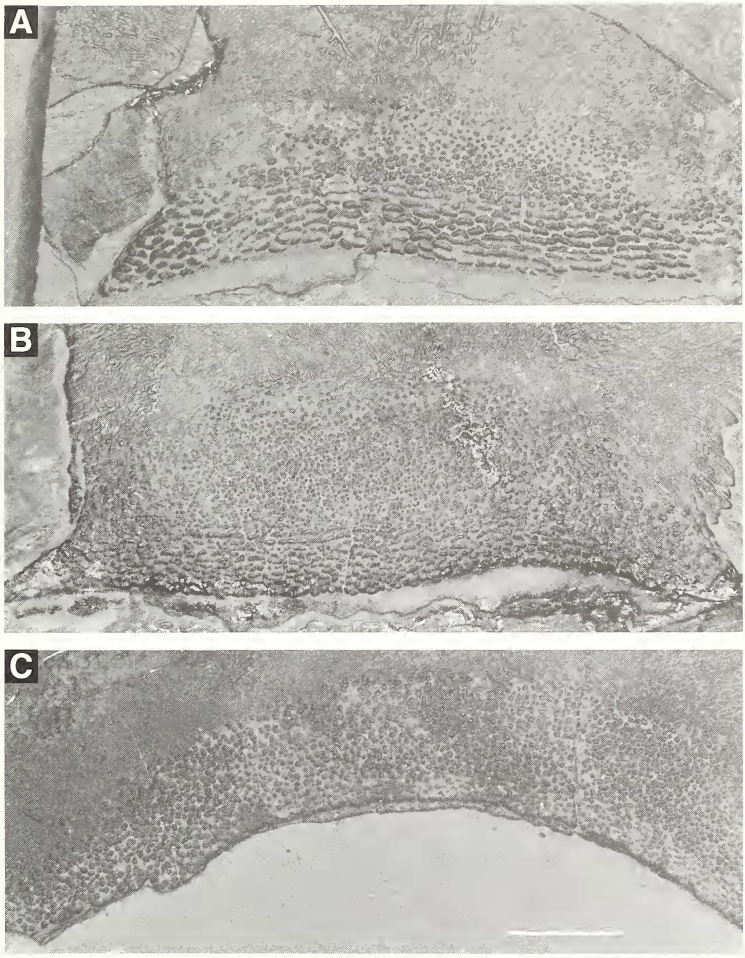

Figure 7. *Stenosteus angustopectus* sp. nov. A, sclerotic plate from holotype (CMNH 8042) showing rod-like medial denticles. B, sclerotic plate from CMNH 8044 showing intermediate condition. C, sclerotic plate from CMNH 8045 showing punctate pattern of denticles. Scale bar = 0.5 cm.

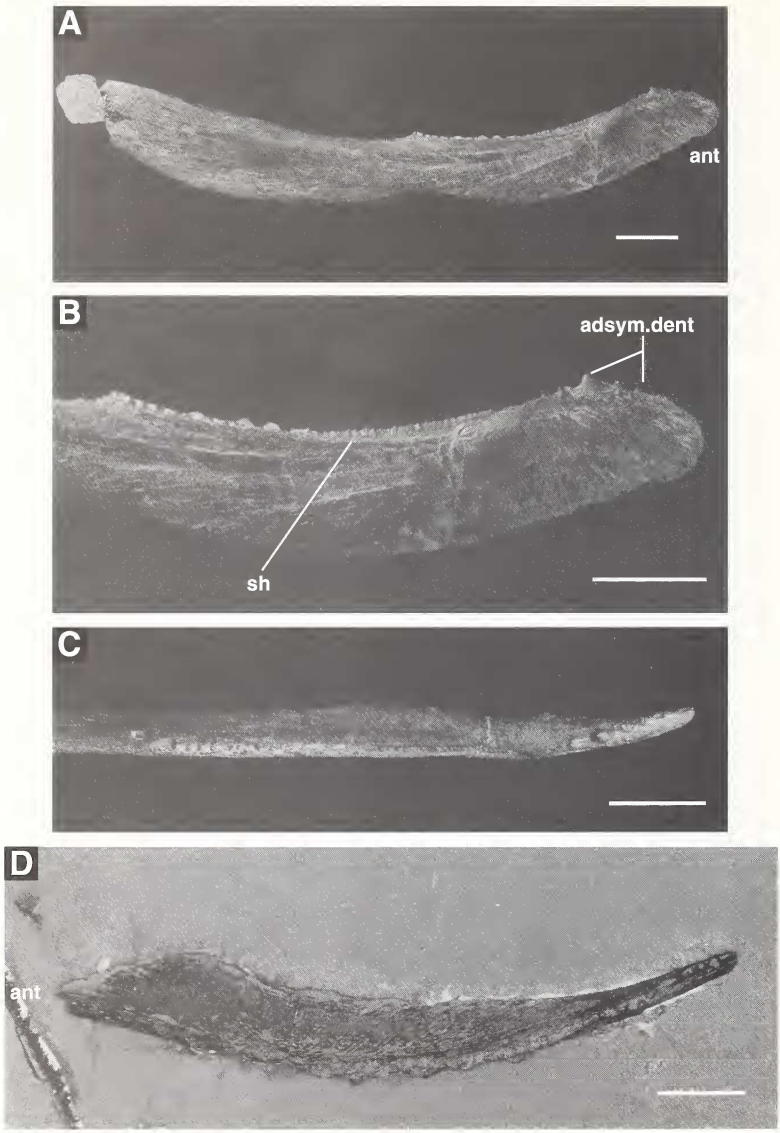

Figure 8. *Stenosteus angustopectus* sp. nov. (CMNH 8042). A, right inferognathal in lateral view and B, a close-up of the occlusal region. C, dorsal view of the occlusal region of the right inferognathal. D, right posterior superognathal in ventral view. A–C, scale bars = 1 cm. D, scale bar = 0.5 cm.

pr.det; see also Dennis and Miles, 1979b, fig. 10). This feature, when present, can be recognized on the dorsal extending ridge of the quadrate as a "stout, forward pointing process situated above the posterior end of the condylar area" (Stensiö, 1963, p. 236). Dennis and Miles (1979a, fig. 16) also interpreted an unossified area on the quadrate in *Canmropiscis coucinnus* as evidence for the presence of a cartilaginous detent process. Gardiner and Miles (1990, p. 196) consider the detent process to be an eubrachythoracid synapomorphy, but missing (secondarily lost) in *Brachyosteus*, brachydeirids, trematosteids, and leiosteids. Among aspinothoracid arthrodires a detent process is known to be present in *Heintzichthys* (Carr, 1991, fig. 6B). The large number of taxa for which this feature is unknown makes it difficult to critically analyze, although, its known distribution is consistent with the interpretation of Gardiner and Miles (1990).

Submarginal (SM). The submarginal plate (Figures 1B, 6C, 12) is rectangular to oval in shape with the longest dimension paralleling the head shield margin. The plate is narrower anteriorly with the ossification center located posteriorly. An internal groove for the hyomandibula is absent.

The reconstructed position of the submarginal plate based on known plate overlaps (Figure 1B) suggests a possible anterior shift relative to the condition seen in *Gymnotrachelus* (Carr, 1994, fig. 2B). This shift has resulted in the distancing of the suborbital plate from the head shield margin forming a large gap between the head shield and cheek plates.

Sclerotic (scler). Four ornamented sclerotic plates are associated with each eye. The ornament consists of punctate tubercles peripherally that coalesce centrally to form short rod-like tubercles which parallel the plate's central margin. The pattern of coalescence is clearly seen in the holotype (CMNH 8042; Figure 7A) and less so in CMNH 8044 (Figure 7B). CMNH 8045 (Figure 7C) and 8046 lack a coalescing pattern with only punctate tubercles present. The degree of coalescence is not correlated with size (based on a comparison of inferognathal size with the pattern of sclerotic plate ornament).

Gnathal Plates and Parasphenoid

General features. Two paired gnathal elements are present (inferognathal and posterior superognathal plates; Figures 8A–C, and 8D respectively). Anterior superognathal plates are not represented on any of the Cleveland Museum specimens. Fragmented parasphenoids are present in the holotype (CMNH 8042) and CMNH 8043. The parasphenoid does not appear to articulate with the anterior superognathals based on the anterior surface of the parasphenoid.

Inferognathal (IG). The occlusal surface forms approximately one half the total length of the inferognathal (Figures 8A–C). A single row of denticles is found along the occlusal surface in the holotype (CMNH 8042) with other specimens showing increasing wear with age. A narrow shelf (sh,

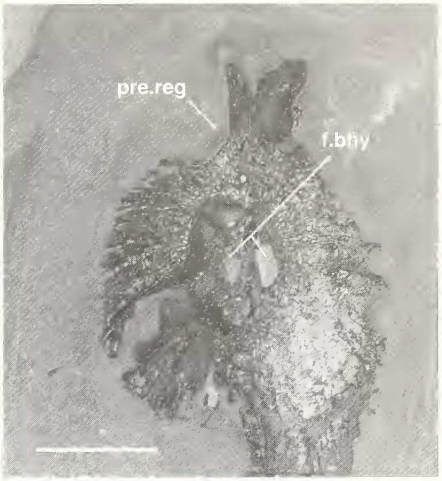

Figure 9. *Stenosteus angustopectus* sp. nov. Parasphenoid plate (CMNH 8043) in ventral view. Scale bar = 0.5 cm.

Figure 8B) is present lateral to the row of denticles. Adsymphyseal denticles (adsym.dent, Figure 8B) are present with the largest typically located at the apex of the adsymphyseal region (type specimen with five or possibly six adsymphyseal denticles on the left inferognathal and four on the right with the most anterior ones missing possibly due to wear). An additional large denticle is present on the occlusal side of the apex. The transition from large denticles to the fine denticles forming the remaining occlusal region is located above the center of ossification. The large denticle forming the apex is assumed to be homologous with the anterior cusp of dunkleosteids. The number of denticles per centimeter varies along the occlusal region with a larger number anteriorly (denticles per centimeter in the holotype, CMNH 8042: 18 per centimeter anteriorly and 10 per centimeter posteriorly).

Posterior superognathal (PSG). The posterior superognathal plate (Figure 8D) is similar in shape to those in *Rhinosteus* (Stensiö, 1963, Pl. 20, figs. 2-3) and *Gymnotrachelus* (Carr, 1994, fig. 9). The posterior superognathals are elongate with a single lateral row of denticles. The denticles are typically worn (denticles per centimeter in the holotype, measured posteriorly only, 12 per centimeter). A distinct medial process is absent. Anteriorly, a medial shelf is developed which gently tapers until it is lost just before the posterior border. In *Gymnotrachelus*, a distinct step is seen separating anterior and posterior regions; however, this feature is absent in *Stenosteus angustopectus*. In

Figure 10. *Stenosteus angustopectus* sp. nov. Median dorsal plate (CMNH 8046) in external view. Scale bar = 1 cm.

further contrast with *Gymnotrachelus*, the originally horizontal posterior shelf is rotated 90° forming a vertical wall with denticles along its ventral border. *Selenosteus brevis* possesses accessory denticles on the posterior portion of the posterior superognathal plate.

The posterior superognathal of *Melanosteus* differs from that in *Stenosteus angustopectus* and *Gymnotrachelus* in being a much deeper structure with a thickening or concentration of denticles located at the apex of the ventral angle (Lelièvre et al., 1987, Pl. 3 [figs. D, E]). Additional denticles are visible along the ventrolateral margin. In contrast, the dorsoventrally flattened posterior superognathals in *Stenosteus angustopectus* and *Gymnotrachelus* possess a series of denticles evenly distributed along their lateral margins (Figure 8D; Carr, 1994, fig. 9A; it is interesting to note that if figs. D and E [Pl. 3] in Lelièvre et al., 1987, are reinterpreted as dorsal and ventral views respectively, then the posterior superognathals of *Melanosteus* and *Stenosteus angustopectus* would share similar outlines with laterally placed denticles; however, the interpretations of these structures have been reconfirmed by Lelièvre, personal communication).

Parasphenoid (Psp). The parasphenoid is poorly preserved and present in only two specimens (the holotype, CMNH 8042, and CMNH 8043). CMNH 8043 (Figure 9) shows a parasphenoid in ventral view. Paired buccohypophysial foramina (f.bhy, Figure 9) are situated near the center of the plate, although it is not clear that anterior and posterior extensions of the plate are fully represented. A ventral groove is absent. The plate is broadest at the level of the foramina with the prehypophysial region rapidly narrowing to form a stemlike anterior projection. A stemlike prehypophysial region (pre.reg, Figure 9) is reminiscent of the condition seen in *Melanosteus* (Lelièvre et al., 1987, Pl. 2 [figs. C–E]) and *Gymnotrachelus* (Carr, 1994, fig. 9B). A second specimen (the holotype, CMNH 8042) may represent a fragmented parasphenoid in dorsal view. A deep buccohypophysial depression is present with the lateral walls of the depression deeply notched. Anterior and posterior extensions of this second parasphenoid are not preserved.

Dermal Shoulder Girdle

General features. The dermal thoracic shield is clearly composed of 15 individual plates (Figures 10–16); three unpaired median plates (median dorsal, anterior median ventral, and posterior median ventral) and six or possibly seven paired plates (anterior dorsolateral, posterior dorsolateral, anterior lateral, posterior lateral, anterior ventrolateral, and posterior ventrolateral, with a possible presence of interolateral plates). The spinal plates are not present in any of the *Stenosteus* material and are assumed to have been lost phylogenetically. Interolateral plates are not recognized in any of the specimens. It is not clear how the lateral and ventral portions of the thoracic shield are interconnected and whether the interolateral plates are either phylogenetically

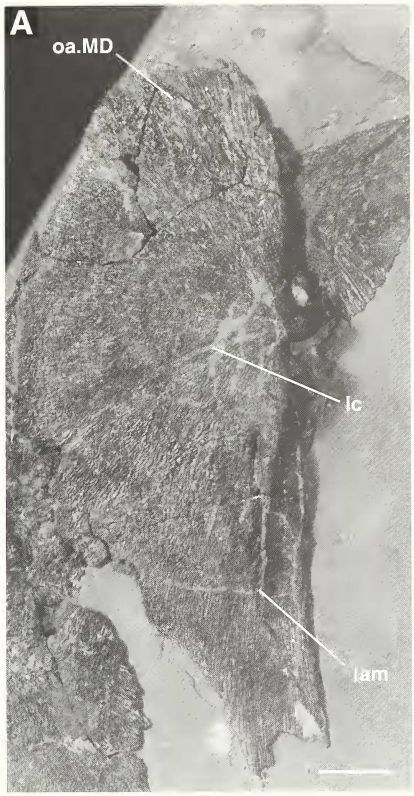

Figure 11. *Stenosteus angustopectus* sp. nov. Right anterior dorsolateral plate in A, external (CMNH 8042) and B, internal (CMNH 8043) views. Scale bars = 1 cm.

lost or just missing from available material (in *Gyaurotrachelus*, only a single putative interolateral plate is preserved which is reduced to a simple elongated plate, Carr, 1994, fig. 11). It should be noted that some aspinothoracid arthrodires, specifically the trematosteids *Parabelosteus* and *Brachyosteus* have lost the interolateral plate (Lelièvre, personal communication; Denison, 1978). The phylogenetic distribution of this feature (loss of the interolateral plates) remains unclear. All plates are secondarily deformed, that is, flattened during diagenesis.

Median dorsal (MD). The median dorsal plate (Figures 1B, 10) of the holotype (CMNH 8042) is incomplete, but shows that the anterior margin is deeply embayed. CMNH 8045 and 8046 (Figure 10) possess a narrow anterior medial process. This process is not supported by an internal keel. The anterolateral margins are slightly notched in the region of the anterior dorsolateral plate and posterior dorsolateral plate contact. The posterior margin is gently embayed in CMNH 8046 and more strongly embayed in CMNH 8045 (a shallow embayment is suggested in the holotype). A non-spatulate carinal process (cr.pr, Figure 10) is visible beyond the posterior edge of the plate in CMNH 8045 and 8046. The internal surface is not exposed in available material.

Anterior dorsolateral (ADL). The anterior dorsolateral plates (Figures 1B, 11) are subrectangular in outline with a deeply embayed ventral margin (height/width = *ca.* 2.8). The anterior dorsolateral plate is overlapped by the median dorsal plate (oa.MD, Figure 11A) with a short process extending anterior to the median dorsal plate and forming part of the nuchal gap border. Ventrally, there is an overlap area for the anterior lateral plate (oa.AL, Figure 11). Anteriorly, the anterolateral overlap area possesses a posteriorly directed lamina (lam, Figure 11A) forming a

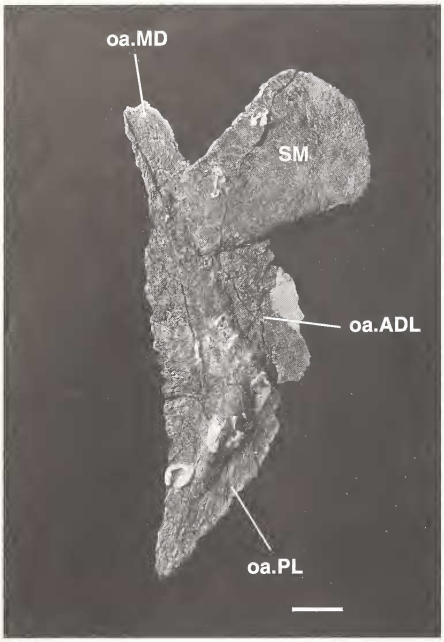

Figure 12. *Stenosteus angustopectus* sp. nov. Right posterior dorsolateral plate (CMNH 8044) in external view. Scale bar = 1 cm.

groove beneath. Apparently, a medial lamina on the anterolateral plate forms a tongue-in-groove junction with the anterior dorsolateral plate. The anterodorsal surface of the flange forms part of the postbranchial embayment.

A continuation of a groove for the main sensory line (lc, Figure 11A) extends to about midplate. The groove is directed posteroventrally (Figure 11A), although its ventral projection is less than that seen in the ventral groove of the main lateral line in coccosteomorph arthrodires (lc.vl of Miles, 1971, fig. 108). Both a glenoid condyle (kd, Figure 11B) and subglenoid process (pr.sg, Figure 11B) are well developed and form part of a strong articulation between the head and thoracic shields.

Posterior dorsolateral (PDL). The posterior dorsolateral plate (Figures 1B, 12) is crescent shaped with a serrate posterior margin (CMNH 8042, length/width = *ca.* 3.1 with the length measured along the greatest dimension and the width perpendicular to length). The external plate face shows three overlap areas: a median dorsal plate

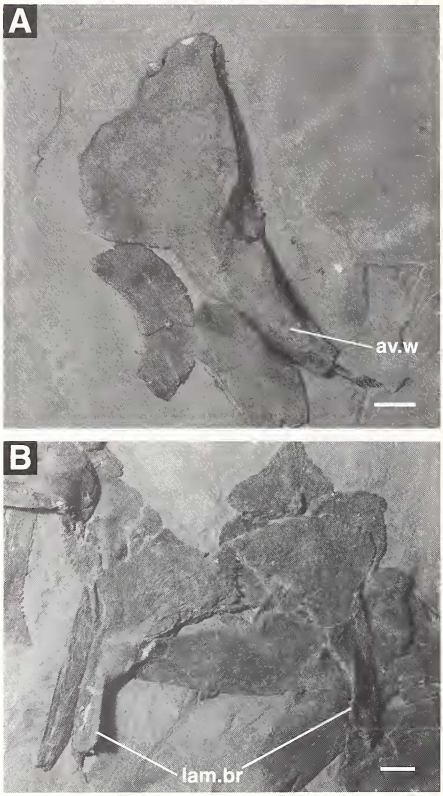

Figure 13. *Stenosteus angustopectus* sp. nov. A, right anterior lateral plate (CMNH 8042) in external view. B, right and left anterior lateral plates (CMNH 8043) in internal view. Scale bars = 1 cm.

overlap (oa.MD, Figure 12), an anterior dorsolateral plate overlap (oa.ADL, Figure 12), and a posterior lateral plate overlap (oa.PL, Figure 12). There is no extension of a lateral line groove onto the plate. Only a dorsal fragment of the posterior dorsolateral plate is exposed on the holotype (CMNH 8042).

Anterior lateral (AL). The anterior lateral plate (Figures 1B, 13) is triangular in outline with the external anteroventral wing (av.w, Figure 13A) tapering to its ventral end. The broader dorsal region and ventral region form an angle of *ca.* 145° along the anterior margin (*ca.*

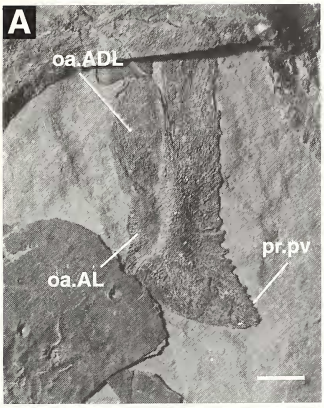

Figure 14. *Stenosteus augustopectus* sp. nov. (CMNH 8043). A, left posterior lateral plate in external view. B, anterior median ventral plate in internal view. Scale bars = 1 cm.

135° in CMNH 8044 and in CMNH 8043 *ca.* 140° on the right and *ca.* 156° on the left, although these latter two estimates are based on internal views). Dorsally, the anterior margin consists of two laminae. The medial lamina forms a tongue-in-groove joint with the anterior dorsolateral plate. The external lamina does not appear to extend beyond the anterior edge of the anterior dorsolateral plate, thus, the anterior lateral plate lacks a distinct obstantic process overlying the postbranchial embayment, which houses the posterolateral margin of the head shield. Internally, a well-developed branchial lamina is present (lam.br, Figure 13B).

Posterior lateral (PL). The posterior lateral plate (Figures 1B, 14A) is not exposed on the holotype (CMNH 8042), but is rhomboidal in outline with the posteroventral corner forming a short process (pr.pv, Figure 14A). This process is directed posteroventrally forming part of the pectoral fenestra border. A similar situation is seen in *Heintzichthys gouldii* (Carr, 1991, figs. 2, 10B); although, the process is much more elongate in *Heintzichthys*.

Table 2. A data matrix for the taxa and characters used in the current analysis (11 taxa, 18 characters, (?) = missing data, (–) = cases where the character is not applicable).

Trematosteidae	1 1 0 1 0	0 0 0 0 0	0 0 0 0 0	1 2 ?
Brachydeiridae	1 0 2 1 0	0 0 1 0 0	0 0 1 0 ?	0 1 ?
Gymnotrachelus	1 – 0 0 1	1 1 0 0 1	1 1 0 1 0	0 2 0
Euseosteus	1 0 2 0 1	1 1 0 1 0	0 0 ? 0 1	0 0 ?
Microsteus	1 0 2 0 1	1 1 0 1 0	0 1 1 0 1	0 0 ?
Pachyosteus	1 0 2 0 1	1 1 0 0 1	0 0 1 0 ?	0 0 0
Rhinosteus	1 0 2 0 1	1 1 0 0 1	1 1 1 0 ?	1 0 1
Melanosteus	? 0 ? 0 1	1 1 0 0 1	1 1 0 1 1	1 0 0
Brannosteus	? 1 1 0 0	0 0 0 0 0	0 0 1 0 ?	0 ? –
Stenosteus augustopectus sp. nov.	1 0 1 0 1	1 1 0 0 1	1 1 0 1 0	1 1 1
Seleurosteus brevis	1 0 ? 0 1	? 1 0 0 1	1 1 0 ? ?	0 1 1

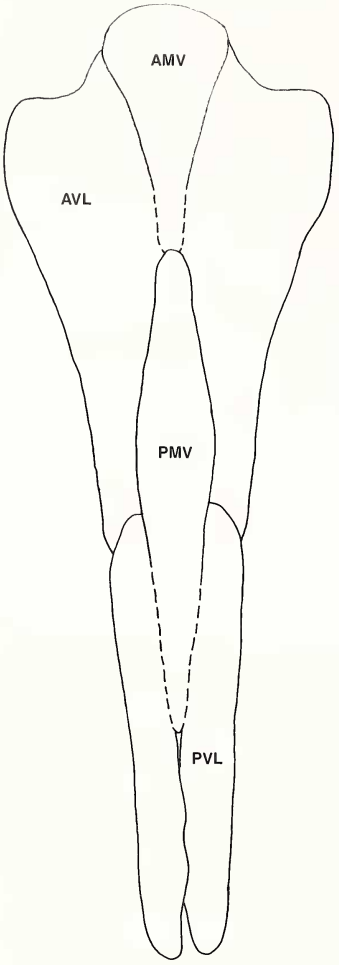

Figure 15. *Stenosteus angustopectus* sp. nov. A reconstruction of the ventral thoracic shield in dorsal view. Based on photographic tracings from CMNH 8042 (left AVL, left PVL, and PMV) and CMNH 8043 (AMV). Right elements are based on mirror images of the two left elements in CMNH 8042. The relationship of the AMV to neighboring bones is speculative due to a lack of visible overlap areas. Visible plate outlines are shown as solid lines. Visible reconstructed plate boundaries are shown as dashed lines.

Overlaps for the anterior lateral (oa.AL, Figure 14A), anterior dorsolateral (oa.ADL, Figure 14A), and posterior dorsolateral plates are present, although the latter is not distinct.

Interolateral (IL). The interolateral plate is missing in all the Cleveland Shale *Stenosteus* and *Selenosteus* specimens. The articular relationships between the branchial lamina of the anterior lateral plate, the anterior ventrolateral plate, and the anterior median plate remain obscure. There is no evidence, e.g., of overlap areas for direct anterior lateral plate articulation with the ventral shield, that would support the phylogenetic loss of the interolateral plate.

Anterior median ventral (AMV). An anterior median ventral plate is recognized in CMNH 8043 only and is exposed in internal view (Figures 14B, 15). The plate is triangular in outline with the base anterior (length/width at base = *ca.* 1.6). Bilateral shallow depressions on the internal surface (Figure 14B) may suggest the presence of overlap areas on the external surface (depressed during preservation).

Posterior median ventral (PMV). The posterior median ventral plate is incompletely preserved (Figures 15, 16A). The length of the preserved portion is *ca.* 73% of the total posterior ventrolateral plate length and *ca.* 59% of the medial length of the anterior ventrolateral plate. Externally, there are overlap areas for the anterior and posterior ventrolateral plates (oa.AVL and oa.PVL respectively, Figure 16A). Internally, a midline groove is present (gr, Figure 16C).

Anterior ventrolateral (AVL). The anterior ventrolateral plate (Figures 15, 16C) is elongate (median length/maximum width = *ca.* 3.6) with its greatest width anterior. The anterior ventrolateral plate tapers from its widest point to the posterior border with the lateral margin slightly concave. Anteriorly, there is a narrow medial process (pr., Figure 16C), which appears to extend the ventral shield well under the head.

Posterior ventrolateral (PVL). The posterior ventrolateral plate (Figures 15, 16B, C) is elongate, being over eight times longer than wide (length/width = *ca.* 8.4 in CMNH 8042). The ossification center is located approximately one-third the length of the plate from the plate's posterior border. An overlap area for the anterior ventrolateral plate (oa.AVL, Figure 16B) is present on the external surface and is located off-center with the distance to the medial edge being greater than that to the lateral edge.

Pectoral and Pelvic Fins, Axial Skeleton, and Neurocranium

The pelvic fins, axial skeleton, and neurocranium are not preserved. A single fragmentary scapulocoracoid (Figure 17) is preserved. Various, but poorly preserved perichondral ossifications are present. The scapulocoracoid (scap, Figure 17) is perichondrally ossified. The margin is incomplete; however, the scapulocoracoid appears to be taller than long. Muscle scars are restricted to the region of the pectoral crest. Numerous neurovascular canals are noted; however, homologies of individual canals are unclear.

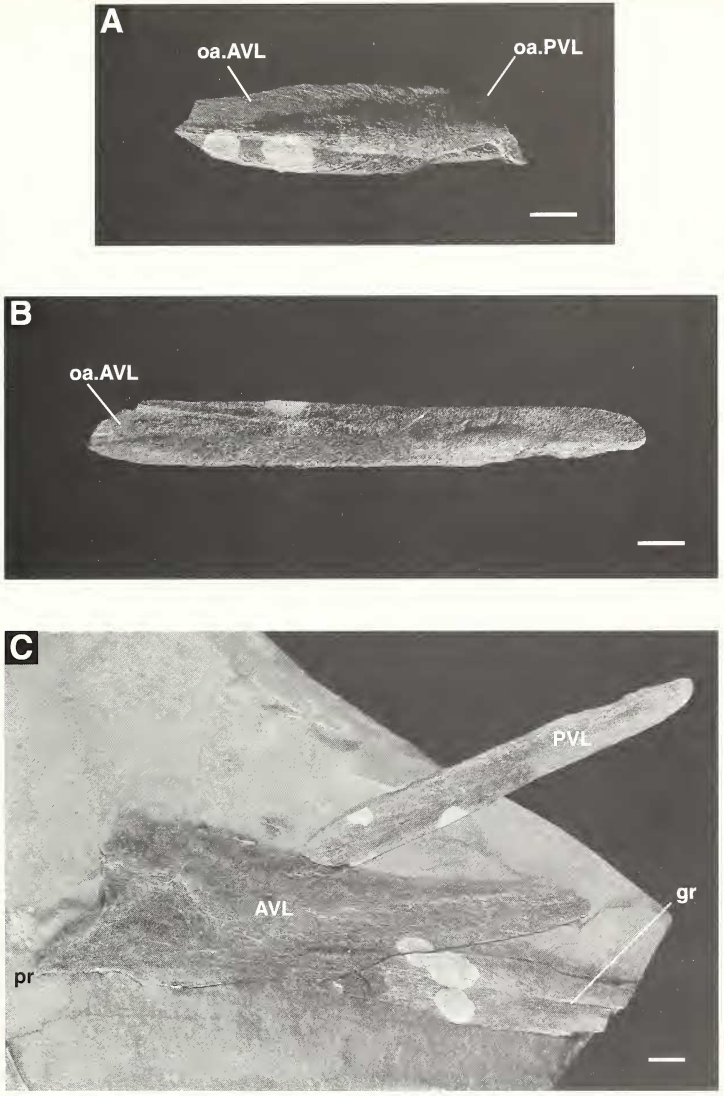

Figure 16. *Stenosteus angustopectus* sp. nov. (CMNH 8042). A, posterior median ventral plate in external view. B, left posterior ventrolateral plate in external view. C, right anterior ventrolateral, left posterior ventrolateral, and posterior median ventral plates in internal view. Scale bars = 1 cm.

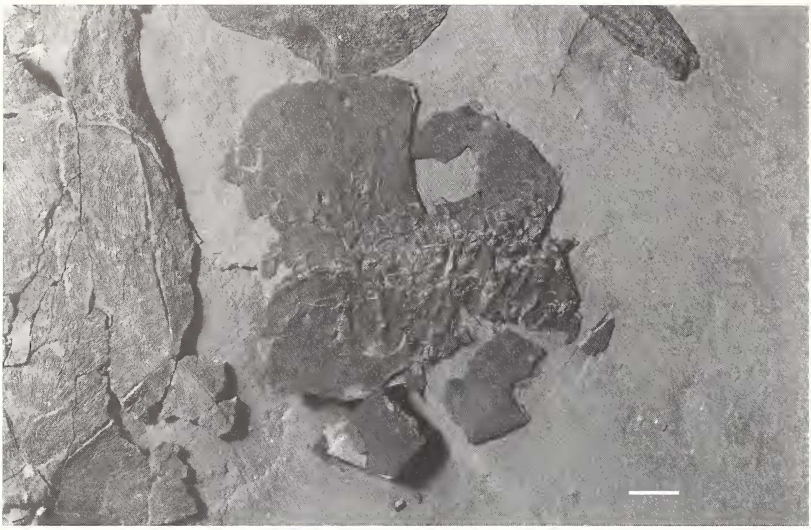

Figure 17. *Stenosteus angustopectus* sp. nov. Perichondrally ossified scapulocoracoid (CMNH 8043) in lateral view. Scale bar = 1 cm.

Systematics Discussion

Phylogenetic analysis

Phylogenetic hypotheses are based on analyses using PAUP (v. 3.1, Swofford, 1993) which uses a parsimony argument to choose between alternative hypotheses of relationships (see Kluge, 1984, for a discussion of the application of parsimony to phylogenetic analyses). Character data and taxa used in the current analysis (Table 2) follow those of Lelièvre et al. (1987) and Carr (1994; *Gymnotrachelus, Melanosteus, Rhinosteus, Pachyosteus, Enseosteus, Microsteus, Braunosteus,* Brachydeiridae, and Trematosteidae) with *Stenosteus angustopectus* and *Selenosteus brevis* added to the study. Finally, diagnostic features of individual clades are based on an *a posteriori* analysis of character distributions (Patterson, 1982).

The current PAUP analysis gives ten equally parsimonious trees (individual treelengths = 31, consistency indices = 0.613), which provides an estimate of relationships based on currently published data, but fails to resolve completely the relationships of *Selenosteus* and *Stenosteus.* In contrast to Lelièvre et al. (1987), Carr (1994), and Gardiner and Miles (1994) the relationships within selenosteid arthrodires become ambiguous with the addition of *Selenosteus* and *Stenosteus* to the analysis. The utility of retaining *Selenosteus* and *Stenosteus* as distinct genera is evaluated subjectively. Many of the diagnostic characters used to distinguish these two genera are missing in related forms thereby resulting in a lack of cladistic resolution. Parameters specified in PAUP include the branch and bound search option with all characters unordered and Trematosteidae set as the outgroup. The most parsimonious trees (minimal character transformations) and their strict consensus (a single tree showing those groups that are present in all eight trees) are retained for discussion.

The choice of outgroups has a minimal effect on the topology within Selenosteidae. All possible combinations of designated outgroups using either two or three non-selenosteid taxa (Trematosteidae, Brachydeiridae, and *Braunosteus*) differ only in the resolution of *Melanosteus.* When Trematosteidae is deleted from the analysis, *Melanosteus* is the sister taxon to an unresolved group (*Stenosteus, Selenosteus,* and *Gymnotrachelus*).

Characters 1–15 are taken from Carr (1994; characters 1–14 originally taken from Lelièvre et al., 1987) with three additional characters added to the current study. The characters are listed below:

1. Submarginal plate shape and orientation (modified from Lelièvre et al., 1987): elongate (0); short (1). Lelièvre et al. (1987, p. 17) consider the derived condition to be raised and reduced ("releveé et réduite"). The primitive condition is an elongate submarginal whose primary axis parallels the head shield margin (e.g., *Dunkleosteus,* Denison, 1978, fig. 69A). A shortened submarginal

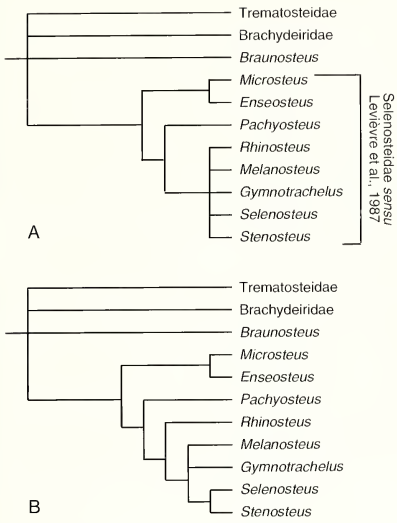

Figure 18. A, a strict consensus tree based on ten trees derived from PAUP (trees found with branch and bound search, treelength = 31, consistency index = 0.613). B, a tree representing the hypothesized relationships discussed in the text. A and B with Trematosteidae designated as the outgroup.

plate, only, is considered here as the derived condition since the character state of Lelièvre et al. (1987) implies both shortening and either elevation, rotation, or both. In *Gymnotrachelus* the submarginal is shortened but the primary axis remains parallel to the head shield margin, whereas, the submarginal appears to be rotated in forms such as *Rhinosteus* (Denison, 1978, fig. 76A) and *Brachyosteus* (Denison, 1978, fig. 74B). A distinct character state of rotation or elevation is not evaluated in the current analysis. To evaluate these features, information is required concerning the exact location of the ossification center which is not readily available.

2. Postnasal plate fused to preorbital plate (Lelièvre et al., 1987): absent (0); present (1). Stensiö (1963, p. 342) interpreted the presence of an interfenestral process on the preorbital plate's dermal preorbital process (pr.if, Stensiö, 1963, fig. 103B) and its association with the course of the supraorbital sensory line groove as evidence for the fusion of the postnasal plate to the preorbital plate. He noted this condition in *Hadrosteus, Brauuosteus, Leiosteus, Errouevuosteus, Belosteus, Trevuatosteus, Cyrtosteus,* and *Brachyosteus* (the latter four taxa are members of the family Trematosteidae). It is not possible at present to distinguish between the fusion of the postnasal and preorbital plates from the loss of the postnasal plate and the independent development of an interfenestral process. The presence of two ossification centers would help to confirm the former hypothesis, although this information is not available in the current analysis.

3. Marginal plate forms part of orbit margin (modified from Lelièvre et al., 1987): absent (0); restricted (1); unrestricted (2). This character represents a complex relationship between the head shield and cheek plates. The primitive condition is one where the marginal plate plays no part in forming the orbit border (e.g., *Dunkleosteus,* Denison, 1978, fig. 69A). The marginal plate, when excluded from the orbit or limited to a posterior recess, possesses a straight, convex, or minimally concave lateral edge. Two derived states, involving participation of the marginal plate in the orbit, are recognized. In forms such as *Microsteus* (Denison, 1978, fig. 76D), *Pachyosteus* (Denison, 1978, fig. 76C), *Rhinosteus* (Denison, 1978, fig. 76A), and brachydeirids (Denison, 1978, figs. 56B–D) the lateral edge of the marginal plate, in forming the posterior orbit margin, is strongly concave (the ventral margin is directed anteriorly in the latter two taxa). In all these forms and in *Enseosteus,* the suborbital plate is in close approximation with the marginal plate (a suborbital-marginal plate contact is seen in *Rhinosteus, Enseosteus,* and brachydeirids). A consequence of the above derived condition is a change in the head shield's outline along the posterior ventrolateral corner (the corner or angle formed by a line from the para-articular process to the postmarginal plate and a line from the postmarginal plate to the orbit margin at the level of the marginal-postorbital plate contact). The primitive condition is a V-shaped ventrolateral corner. In the taxa above, possessing a marginal plate involvement in the orbit, the anterolateral edge of the ventrolateral corner possesses a distinct angulation resulting in the posterior orbit border paralleling, or nearly so, the posterolateral edge of the head shield corner (a condition representing an unrestricted involvement of the marginal plate in the orbit).

The marginal plate in *Steuosteus augustopectus* participates in the orbit margin, but is located within a posteriorly directed recess. The head shield retains a primitive V-shaped outline for the ventrolateral corner (a restricted involvement of the marginal plate in the orbit). A transitional condition between no involvement in the orbit margin and the marginal plate bordering an open posterior recess is seen in *Gymnotrachelus* where a small gap extends from the orbit between the head shield and cheek plates (Carr, 1994, p. 11, fig. 2B).

Due to the complexity of these features, it is important in all cases to compare the relationship of the suborbital, posterior suborbital, and submarginal plates to clearly determine if the marginal plate is involved in the orbit margin. Among taxa where known, the internal supraorbital crista is restricted to the postorbital plate or as noted in this case extends only a limited distance onto the marginal plate. The posterior extent of this feature does not appear to be a good indicator of marginal plate involvement in the orbit border (see Stensiö, 1963, figs. 112A, B, 113A–C and Lelièvre et al. 1987, fig. 3).

4. Position of the preorbital-postorbital-central plate junction (Lelièvre et al., 1987): at a level over the anterior half of the orbit (0); posterior half of orbit (1).
5. Angle formed by the postorbital and otic branches of the infraorbital sensory line grooves (Lelièvre et al., 1987): open (0); closed (1). Gardiner and Miles (1994) noted that an angle of less than 45° is restricted to *Selenosteus* and the European selenosteids with the condition in *Gymnotrachelus* being transitional. Carr (1994) reinterpreted the relationship of these sensory lines in *Gymnotrachelus*, noting an angle of *ca.* 30–40°.
6. Length of cheek and head shield contact, independent of overlapping or fusion of these two dermal units (Lelièvre et al., 1987): long (0); short (1).
7. Nature of inferognathal and posterior superognathal occlusal surfaces (Lelièvre et al., 1987): trenchant or rounded (0); denticulate (1).
8. Posterior ventrolateral and posterior median plates (Lelièvre et al., 1987): present (0); absent (1).
9. Position of the dermal articulation between the head and thoracic shields (modified from Lelièvre et al., 1987): dorsolateral (0); displaced ventrally (1).
10. Dorsal process on the posterior superognathal plate (Lelièvre et al., 1987): present (0); absent (1).
11. Form of the anterior lateral plate (Lelièvre et al., 1987): infraobstantic region of plate short (0); infraobstantic and postbranchial region elongate with the dorsal region narrow (1).
12. Linguiform process on the suborbital plate (modified from Lelièvre et al., 1987): present (0); reduced (1). This character has been scored as in Lelièvre et al. (1987), although absence of a linguiform process is reinterpreted here as a reduction. The presence of a linguiform process may represent a plesiomorphic feature for the aspinothoracid arthrodires. Recognition of this process in lateral view may reflect the size of the subautopalatine crista (cr.sau, Figure 5B; Carr, 1991) and whether, when secondarily flattened during preservation, the process extends below the ventral external border of the suborbital plate. This crista is often thin and easily lost unless reinforced to form a contact face with the posterior superognathal as seen in *Dunkleosteus* and *Eastmanosteus calliaspis* (cf.PSG, Carr, 1991, fig. 7B).
13. Overlap between the head and cheek dermal plates (Lelièvre et al., 1987): absent (0); present (1). Lelièvre (personal communication) reinterprets this character in *Melanosteus* as being absent (0), i.e., lacking an overlap, based on his interpretation of the lateral border of the head shield (see Lelièvre et al., 1987, fig. 3, Pl. 1 [figs. A–C]).
14. Prehypophysial region of parasphenoid plate elongate and stem-like (modified from Lelièvre et al., 1987): absent (0); present (1).
15. Supraethmoid thickening (th.seth, Stensiö, 1963, figs. 113A, B): absent (0); present (1).
16. Marginal and central plate contact: absent (0); present (1).
17. Length ratio of parasagittal dimensions of preorbital and central plates (PrO/C; Denison, 1978): $x < 0.75$ (0); $0.75 < x < 1.25$ (1); $x > 1.25$ (2).
18. In forms with a denticulate inferognathal, the nature of the denticle pattern: multiple rows (0); single fine row (1).

Selenosteidae Dean, 1901

Dean (1901) originally described the family Selenosteidae, in which he included *Selenosteus, Stenosteus, Diplognathus,* and possibly *Callognathus.* He characterized the group based on the presence of a denticulate inferognathal, adsymphysial denticles, large orbits, a lack of a postorbital process, a nuchal plate with a deep posterior embayment, a well-developed articulation between the head and thoracic shields, and the median dorsal plate shape with reduction of the carinal process and associated keel.

Denison (1978) characterized the family by the presence of large orbits, long centrals (relative to preorbitals), short submarginal plates, and a large nuchal gap. He united within the family a number of European taxa (*Brannosteus, Enseosteus, Microsteus, Pachyosteus,* and *Rhinosteus*) and North American taxa (*Gymnotrachelus, Paramylostoma, Selenosteus,* and *Stenosteus*). He noted differences between these two geographically separate faunas, although he did not provide a phylogenetic analysis.

Lelièvre et al. (1987), added *Melanosteus* to the family and suggested that the brachydeirid arthrodires and Selenosteidae are sister taxa (Figure 18A). They excluded *Brannosteus* from Selenosteidae and did not analyze *Paramylostoma, Selenosteus,* or *Stenosteus.* Gardiner and Miles (1994) also recognized a sister group relationship between *Gymnotrachelus* and European selenosteids (*Selenosteus* was not included in their analysis) although their proposed relationships among European selenosteids differ from that of Lelièvre et al. (1987). Following Lelièvre et al. (1987), Carr (1994) reevaluated the relationships of *Gymnotrachelus,* but excluded *Selenosteus* and *Stenosteus* from his analysis and considered the relationship of *Brannosteus* unresolved.

Lelièvre et al. (1987), Carr (1994; Figure 18), and Gardiner and Miles (1994) agree that Selenosteidae (exclud-

Table 3. The left column provides a summary of the plates identified and doubtful structures discussed by Dean (1901) for *Stenosteus glaber* AMNH 7313. Quotes are used to denote archaic terminology or specific phrases used by Dean. Page and plate references refer to discussions in Dean (1901). The right column provides a current interpretation of these structures. Caution should be taken in analyzing Dean's original figures. The lithographic method employed by Dean reproduced the figures as mirror-images, a problem common to lithography (Griffiths, 1980, p. 101, figs. 89, 90).

Bones discussed by Dean (1901)	current interpretation
"Median occipital" (Nu) (p.89; Pl. IV, fig. 19)	present
Central (C) (p. 89; Pl. III, fig. 4)	present
Marginal (M) (p. 89; Pl. III, figs. 3c, 4)	present
"External occipital" (PNu) (p. 90; Pl. III, fig. 4)	present
Postorbital (PtO) (p. 90; Pl. III, figs. 3b, 4)	present
Preorbital (PrO) (p. 90; Pl. IV, fig 11)	present
Rostral (R) (p. 90; Pl. III, fig. 5)	= SM? (possible R can be seen between Psp and AL)
Pineal (P) (p. 90; Pl. IV, fig. 22)	= Psp
(?P, Pl. III, fig. 2)	= AMV?
"Mandible" (IG) (p. 91; Pl. IV, figs. 15, 17)	present
"Maxillaries" (PSG) (p. 91; Pl. IV, figs. 14, 14A)	present
"Premaxillaries" (ASG) (p. 92; Pl. IV, fig. 13)	present
Suborbital (SO) (p. 92; Pl. IV, figs. 12, 18)	present
Sclerotic (scler) (p. 92; Pl. III, figs. 7, 8, 10)	present (only 8 present)
Median dorsal (MD) absent ("no trace," p. 93)	present (impression only, next to PMV)
Anterior dorsolateral (ADL) (p. 93; Pl. IV, fig. 16)	present
Posterior median ventral (PMV) (p. 93; Pl. IV, fig. 20)	present
Anterior median ventral (AMV) (p. 93)	present
(AVL) (p. 93; Pl. III, fig. 6)	? (possible AL)
(PVL) (p. 93; Pl. III, fig. 9)	? (possible AVL)

Doubtful plates discussed by Dean (1901)	current interpretation
Pl. III, fig. 3 (p. 90)	"a" = ?Marginal (due to presence of a short pmc)
	"b" = Postorbital
	"c" = Marginal
Pl. IV, fig. 22 (p. 90)	"Pi" = Parasphenoid
Pl. III, fig. 1 (p. 91)	= Pineal
Pl. III, fig. 2 (p. 91)	= AMV?

Plates not discussed by Dean (1901)	current interpretation
PL	present
PDL	present

ing *Braunosteus*) are characterized by: (1) enlarged orbits (character 5, Lelièvre et al., 1987; characterized by changes in the sensory line patterns associated with enlarged orbits), (2) a reduced cheek–head shield contact (character 6, Lelièvre et al., 1987), and (3) inferognathals and posterior superognathals possessing occlusal denticles (character 7, Lelièvre et al., 1987). An anterior shift of the preorbital-postorbital-central plates triple junction unite Selenosteidae *sensu* Denison (1978), although the distribution of this character is equivocal when evaluating Selenosteidae *sensu* Lelièvre et al. (1987, Brachydeiridae as the sister group to Selenosteidae excluding *Braunosteus*). The distribution of short submarginal plates (a

Table 4. The left column provides a summary of the plates identified and doubtful structures discussed by Dean (1901) for *Selenosteus brevis* AMNH 7312. Quotes are used to denote archaic terminology or specific phrases used by Dean. Page and plate references refer to discussions in Dean (1901). The right column provides a current interpretation of these structures. Caution should be taken in analyzing Dean's original figures. The lithographic method employed by Dean reproduced the figures as mirror-images, a problem common to lithography (Griffiths, 1980, p. 101, figs. 89, 90).

Bones discussed by Dean (1901)	current interpretation
"Median occipital" (Nu) (p. 94; Pl. VI, fig. 33)	present
Central (C) (p. 94; Pl. VI, fig. 33)	present
Marginal (M) (p. 95; Pl. VI, fig. 33)	present
"External occipital" (PNu) (p. 95; Pl. VI, fig. 33)	present
Postorbital (PtO) (p. 96; Pl. VI, fig. 33)	present
Preorbital (PrO) (p. 96; fig. 1; Pl. VI, fig. 33)	present
Rostral (R) absent (p. 96)	absent
Pineal (P) absent (p. 96)	absent
"Mandible" (IG) (p. 96; Pl. VI, figs. 36, 37)	present
"Premaxillary" (ASG) absent (p. 94)	absent
"Maxillary" (PSG) absent (p. 94)	present
Suborbital (SO) (p. 97; Pl. VI, fig. 35)	present
Sclerotic (scler) (p. 97; Pl. VI, fig. 34)	present
Median dorsal (MD) (p. 97; Pl. V, fig. 23)	removed by Dean
Anterior dorsolateral (ADL) (p. 97; Pl. V, fig. 32)	present
Posterior dorsolateral (PDL) (p. 97; "not present ... unless ... shown in Pl. V, fig. 27")	absent?
Anterior ventrolateral (AVL) (p. 97; Pl. V, fig. 28)	present
Posterior ventrolateral (PVL) (p. 98; Pl. V, fig. 25)	present
Anterior median ventral (AMV) absent (p. 98)	absent
Posterior median ventral (PMV) (p. 98; Pl. V, fig. 26)	present
Integument (p. 99; Pl. V, fig. 24)	=Scapulocoracoid
(p. 99; Pl. V, fig. 31)	=perichondral ossification
Doubtful plates discussed by Dean (1901)	**current interpretation**
Pl. VI, fig. 33, X (p. 98) "preorbital"	?
Pl. VI, fig. 38 (p. 98) "clavicular" or "anterolateral"	=Anterior lateral
Pl. V, fig. 28A & Pl. V, fig. 30 (p. 98)	=Posterior suborbital
Pl. V, fig. 28B & Pl. V, fig. 29 (p. 98)	=Submarginal?
Pl. V, fig. 27 "interolateral" (p. 98)	=Posterior lateral
Plates not discussed by Dean (1901)	**current interpretation**
PL	present
PSO	present
SM	present
scapulocoracoid	present

Table 5. Characters suggesting distinctness of the genera *Selenosteus* and *Stenosteus*. The phylogenetic value of these features remains obscure due to missing data and the lack of information concerning original material in related taxa. A final resolution of the validity of these genera and their relationship within Selenosteidae is beyond the scope of the current study; however, the current analysis provides a basis for their retention.

Selenosteus	*Stenosteus glaber* and *S. angustopectus*
lacks a central-marginal plate contact	central-marginal contact present (Dean, 1901)
intricate marginal-paranuchal plate joint	simple plate joint (Dean, 1901)
reduced lateral paranuchal ala along the plate's posterior border	laterally expanded paranuchal ala
anterior paranuchal ala extends far forward	reduced anterior extension (Dean, 1901)
shallow concavity on ventral margin of the anterior dorsolateral plate	accentuated concavity
concave posterior margin on the paranuchal lateral to the para-articular process	transverse posterior margin
accessory denticles along posterior aspect of the posterior superognathal plate	single row of denticles

selenosteid character used by Denison, 1978) has been shown to be a plesiomorphic feature of Selenosteidae (Lelièvre et al., 1987). The presence of a marginal–central plate contact (suggested selenosteid character, Dean, 1901) represents a derived feature within Selenosteidae (*Stenosteus, Rhinosteus,* and *Melanosteus*). The median dorsal plate shape and reduction of the carinal process and associated keel (Dean, 1901) additionally represent derived features within Selenosteidae seen in *Gymnotrachelus, Selenosteus brevis,* and *Stenosteus angustopectus.*

The confusion concerning family membership and the exclusion of taxa in analyses is a result, in part, of a lack of morphological information for various North American taxa. Additionally, *Selenosteus* and *Stenosteus* have not been reevaluated since Dean's (1901) original report leaving the published descriptions inadequate and in error. The description of *Stenosteus angustopectus* provides useful comparative material to reevaluate the type specimens of *Selenosteus brevis* and *Stenosteus glaber.* Tables 3 and 4 provide a current reinterpretation of the individual bones discussed and figured by Dean (1901).

Within Selenosteidae (Figure 18B), *Selenosteus* and *Stenosteus* are united by the presence of a single row of finely spaced denticles along the inferognathal occlusal surface (Character 18) and a reduction in the central plate length relative to the preorbital plate (PrO/C ratio is subequal, Character 17). The first character above represents a subjective comparison based on figures of potential sister and outgroup taxa (i.e., *Rhinosteus,* Stensiö, 1963, Pl. 20 [fig. 1]; *Gymnotrachelus,* Carr, 1994, fig. 9; *Melanosteus,* Lelièvre, personal communication). The second character is distinct from the plesiomorphic state of elongate central plates with *Gymnotrachelus* representing a derived condition of elongate preorbital plates. The polarity of character transformations from the plesiomorphic state (elongate central plates) to the two derived states (subequal central and preorbital plates and elongate preorbital plates) is unclear.

Carr (1994, fig. 13) united *Melanosteus* and *Gymnotrachelus* based on the presence of a stem-like prehypophysial region of the parasphenoid plate. This feature is also present in *Stenosteus angustopectus*, but unknown in *Stenosteus glaber* and *Selenosteus.* The presence of this process along with the relationship between *Selenosteus* and *Stenosteus* suggests a close relationship between these later two taxa, *Melanosteus,* and *Gymnotrachelus* (Figure 18). These four taxa additionally share a loose connection between the dermal cheek and head shield (Character 13); however, the exact nature of the relationships among these taxa remains unresolved.

Selenosteus *and* Stenosteus

Dean (1901) recognized AMNH 7312 and AMNH 7313 as two distinct genera, *Selenosteus* and *Stenosteus* respectively. He stated (p. 100) that "in differentiating *Stenosteus* as a genus stress has been laid upon its unlikeness to *Selenosteus* in the elements figured in Pl. III, figures 4, 6, 9, and in Pl. IV, figures 11, 21, 22." Dean's (1901) plate interpretations are updated in Tables 3 and 4 with Table 5 providing a summary of differences between these two genera. The phylogenetic value of these differences remains obscure due to missing data and the lack of published information concerning specific characters in related taxa. A final resolution of the validity of these genera and their relationship within Selenosteidae is beyond the scope of the current study.

Stenosteus is characterized by the presence of (1) a narrow laterally extending ala on the paranuchal plate along its posterior border, (2) a reduced anterior extension of the anteromedial part of the paranuchal plate (Dean, 1901), and

(3) a developed concave ventral border of the anterior dorsolateral plate. *Selenosteus* is characterized by (1) a convoluted suture between the marginal and paranuchal plates (Dean, 1901), (2) a concavity along the posterior margin of the paranuchal plate lateral to the para-articular process, and (3) the presence of accessory denticles along the posterior aspect of the posterior superognathal plate.

Conclusion

A new selenosteid arthrodire, *Stenosteus angustopectus,* is described from the Cleveland Shale of northern Ohio, U.S.A. Characterizing *Stenosteus angustopectus* are: (1) long and narrow posterior ventrolateral plates, (2) a narrow median process on the anterior ventrolateral plate, (3) a tongue-in-groove joint between the anterior lateral and anterior dorsolateral plates, (4) a posterodorsal process on the suborbital plate, and (5) a posterior superognathal plate lamina that posteriorly is rotated 90°. This material provides the basis for reevaluating Dean's (1901) original descriptions for *Stenosteus glaber* and *Selenosteus brevis.* Dean's figures and identifications of individual bones are reinterpreted with an update provided in Tables 3 and 4. The taxon Selenosteidae is retained *sensu* Lelièvre et al. (1987) and is diagnosed by the presence of large orbits with associated shifts in the sensory line grooves around the orbit and reduction in the contact between the cheek and head shield, and finally by the presence of a denticulate inferognathal occlusal surface. Additional published characters used to unite Selenosteidae are either equivocal, plesiomorphic, or derived relative to the family (respectively: PrO/C ratio, submarginal plate shape, and marginal–central plate contact and median dorsal plate shape). *Selenosteus* and *Stenosteus* are retained as distinct genera and united as sister taxa. Uniting these taxa are the pattern of denticulation along the inferognathal and a reduction of the relative length of the central plates. A number of characters distinguish *Selenosteus* and *Stenosteus* (summarized in Table 5), although their phylogenetic value is obscured by missing data and incomplete published accounts of related taxa. Finally, diagnoses are provided for *Selenosteus* and *Stenosteus* based on current knowledge of the taxa analyzed in this study.

It is important to the understanding of aspinothoracid phylogenetic relationships that North American taxa continue to be reanalyzed. The Cleveland Shale fauna is a key element since the recovery of a wealth of material during the Interstate 71 Paleontological Salvage Project provides both new taxa and important comparative material for the analysis of poorly known forms. It is equally important to reevaluate much of the Wildungen material discussed and described by Stensiö (e.g., Stensiö, 1963) in light of current work. At present, the state of published descriptions limits this process.

The current work on the Cleveland Shale fauna and the description of a new species of *Stenosteus* helps to resolve a number of questions concerning related taxa and provides a step toward understanding the phylogenetic relationships among aspinothoracid arthrodires. Continuing work on this fauna should prove to be valuable.

Acknowledgments

I would like to thank Michael Williams for his continued support, encouragement, and access to The Cleveland Museum of Natural History collections and John Maisey for access to the American Museum of Natural History collections. Gary Jackson (The Cleveland Museum of Natural History) actively participated in discussions and helped in working with the Cleveland collections. Finally, I want to thank Daniel Goujet, Hervé Lelièvre, and Michael Williams for their reviews of this manuscript. This report was submitted in partial fulfillment of the requirements for a Doctor of Philosophy in Geological Sciences in the Horace H. Rackham School of Graduate Studies at The University of Michigan. This research was supported in part by a grant from the Lerner-Gray Fund for Marine Research, American Museum of Natural History, New York.

References

Carr, R. K. 1991. Reanalysis of *Heintzichthys gouldii*, an aspinothoracid arthrodire (Placodermi) from the Famennian of northern Ohio, U.S.A. with a review of brachythoracid systematics. Zoological Journal of the Linnean Society, 103:349-390.

Carr, R. K. 1994. A redescription of *Gymnotrachelus* (Placodermi: Arthrodira) from the Cleveland Shale (Famennian) of northern Ohio, U.S.A. Kirtlandia, 48:3-21.

Dean, B. 1901. Palaeontological notes. I. On two new arthrodires from the Cleveland Shale of Ohio. New York Academy of Sciences. Memoirs, 2(3):87-100.

Denison, R. H. 1978. Handbook of Paleoichthyology. 2. Placodermi. Stuttgart, Gustav Fischer Verlag, 128 p.

Dennis, K. D., and R. S. Miles. 1979a. A second eubrachythoracid arthrodire from Gogo, Western Australia. Zoological Journal of the Linnean Society, 67:1-29.

Dennis, K. D., and R. S. Miles. 1979b. Eubrachythoracid arthrodires with tubular rostral plates from Gogo, Western Australia. Zoological Journal of the Linnean Society, 67:297-328.

Dennis-Bryan, K. D. 1987. A new species of eastmanosteid arthrodire (Pisces: Placodermi) from Gogo, Western Australia. Zoological Journal of the Linnean Society, 90:1-64.

Dunkle, D. H., and P. A. Bungart. 1939. A new arthrodire from the Cleveland Shale Formation. Scientific Publications of the Cleveland Museum of Natural History, 8:13-28.

Dunkle, D. H., and P. A. Bungart. 1942. A new genus and species of Arthrodira from the Cleveland Shale. Scientific Publications of the Cleveland Museum of Natural History, 8:65-71.

Dunkle, D. H., and P. A. Bungart. 1945. A new arthrodiran fish from the Upper Devonian Ohio Shales. Scientific Publications of the Cleveland Museum of Natural History, 8:85-95.

Gardiner, B. G., and R. S. Miles. 1990. A new genus of eubrachythoracid arthrodire from Gogo, Western Australia. Zoological Journal of the Linnean Society, 99:159-204.

Gardiner, B. G., and R. S. Miles. 1994. Eubrachythoracid arthrodires from Gogo, Western Australia. Zoological Journal of the Linnean Society, 112:443-477.

Griffiths, A. 1980. Prints and Print Making: An Introduction to the History and Techniques. London, British Museum Publications, 150 p.

Heintz, A. 1932. The structure of *Dinichthys:* A contribution to our knowledge of the Arthrodira. Bashford Dean Memorial Volume, Archaic Fishes, 4:115-224.

Kluge, A. 1984. The relevance of parsimony to phylogenetic inference, p. 24-38. *In* T. Duncan and T. F. Stuessy (eds.), Cladistics: Perspectives on the Reconstruction of Evolutionary History. New York, Columbia University Press.

Lelièvre, H., R. Feist, D. Goujet, and A. Blieck. 1987. Les vertébrés dévoniens de la Montagne Noire (sud de la France) et leur apport à la phylogénie des pachyostéomorphes (Placodermes Arthrodires). Palaeovertebrata, 17:1-26.

Miles, R. S. 1971. The Holonematidae (placoderm fishes), a review based on new specimens of *Holonema* from the Upper Devonian of Western Australia. Philosophical Transactions of the Royal Society of London, 263:101-234.

Miles, R. S., and K. D. Dennis. 1979. A primitive eubrachythoracid arthrodire from Gogo, Western Australia. Zoological Journal of the Linnean Society, 65:31-62.

Patterson, C. 1982. Morphological characters and homology, p. 21–74. *In* K. A. Joysey and A. E. Friday (eds.), Problems of Phylogenetic Reconstruction. New York, Academic Press.

Stensiö, E. A. 1963. Anatomical studies on the arthrodiran head. Part I. Preface, geological and geographical distribution, the organization of the head in the Dolichothoraci, Coccosteomorphi, and Pachyosteomorphi. Taxonomic appendix. Kungliga Svenska Vetenskapsakademiens Handlingar, 9:1-419.

Swofford, D. L. 1993. PAUP: Phylogenetic Analysis Using Parsimony, Version 3.1. Computer program distributed by the Illinois Natural History Survey, Champaign, Illinois.

Abbreviations Used in Text and Figures

a.Au	depression for autopalatine
ADL	anterior dorsolateral plate
adsym.dent	adsymphyseal denticles
AL	anterior lateral plate
AMV	anterior median ventral plate
ant	anterior
a.po	postautopalatine crista
AVL	anterior ventrolateral plate
av.w	anteroventral wing
C	central plate
cf.PrO	contact face for preorbital plate
cr.po	postocular crista
cr.pr	carinal process
cr.pso	postocular crista
cr.sau	subautopalatine crista
cr.so	subocular crista
csc	central sensory line groove
d.end.e	external opening for the endolymphatic
f.bhy	paired buccohypophysial foramina
f_e.lv	elongate fossa for levator muscle of head
gr	groove
IG	inferognathal
ioc.ot	otic branch of infraorbital sensory line groove
ioc.pt	postorbital branch of infraorbital sensory line groove
ioc.sb	suborbital branch of infraorbital sensory line groove
kd	glenoid condyle
laf	lateral articular fossa
lam	lamina
lam.br	branchial lamina of AL plate
lc	main lateral line
M	marginal plate
MD	median dorsal plate
n	notch
Nu	nuchal plate
oa.ADL	overlap area for anterior dorsal lateral plate
oa.AL	overlap area for anterior lateral plate
oa.AVL	overlap area for anterior ventrolateral plate
oa.M	overlap area for marginal plate
oa.MD	overlap area for median dorsal plate
oa.PL	overlap area for posterior lateral plate
oa.PNu	overlap area for paranuchal plate
oa.PVL	overlap area for posterior ventrolateral plate
oa.SM	overlap area for submarginal plate
oa.SO	overlap area for suborbital plate
P	pineal plate
pap	occipital para-articular process
PDL	posterior dorsolateral plate
PL	posterolateral plate
PM	postmarginal plate
pmc	postmarginal sensory line groove
PMV	posterior median ventral plate
PNu	paranuchal plate
p.pr	median posterior process
pr	process
pre.reg	prehypophysial region
PrO	preorbital plate
pr.pv	posteroventral process
pr.sg	subglenoid process
PSO	postsuborbital plate
PtO	postorbital plate
PVL	posterior ventrolateral plate
Qu	position of quadrate
R	rostral plate
rec.pr.sv	recess for the supravagal process of the neurocranium
sh	shelf
SM	submarginal plate
SO	suborbital plate
soa	subobstantic area
soc	supraorbital sensory canal groove